



INSTITUT DE FRANCE
Académie des sciences

Comptes Rendus

Chimie

Hester Colboc, Thomas Bettuzzi, Marine Badrignans, Dominique Bazin, Antoine Boury, Emmanuel Letavernier, Vincent Frochot, Ellie Tang, Philippe Moguelet, Nicolas Ortonne, Nicolas de Prost, Saskia Ingen-Housz-Oro and Michel Daudon

Relationship between calcinosis cutis in epidermal necrolysis and caspofungin, a physicochemical investigation


Volume 25, Special Issue S1 (2022), p. 477-487

Published online: 20 July 2022

<https://doi.org/10.5802/crchim.202>

Part of Special Issue: Microcrystalline pathologies: Clinical issues and nanochemistry

Guest editors: Dominique Bazin (Université Paris-Saclay, CNRS, ICP, France), Michel Daudon, Vincent Frochot, Emmanuel Letavernier and Jean-Philippe Haymann (Sorbonne Université, INSERM, AP-HP, Hôpital Tenon, France)

 This article is licensed under the
CREATIVE COMMONS ATTRIBUTION 4.0 INTERNATIONAL LICENSE.
<http://creativecommons.org/licenses/by/4.0/>



*Les Comptes Rendus. Chimie sont membres du
Centre Mersenne pour l'édition scientifique ouverte*
www.centre-mersenne.org
e-ISSN : 1878-1543



Microcrystalline pathologies: Clinical issues and nanochemistry / *Pathologies microcristallines : questions cliniques et nanochimie*

Relationship between calcinosis cutis in epidermal necrolysis and caspofungin, a physicochemical investigation

Hester Colboc^{*,#, a, b}, Thomas Bettuzzi^{#, c, d, e}, Marine Badrignans^f,
Dominique Bazin^{*, g}, Antoine Boury^g, Emmanuel Letavernier^{b, h},
Vincent Frochot^{b, h}, Ellie Tang^b, Philippe Mogueletⁱ, Nicolas Ortonne^e,
Nicolas de Prost^j, Saskia Ingen-Housz-Oro^{c, d, e} and Michel Daudon^{b, h}

^a Sorbonne Université, Hôpital Rothschild, Service Plaies et Cicatrisation, Paris, France

^b UMR_S 1155, Sorbonne Université-UPMC Paris VI, F-75020 Paris, France

^c Service de Dermatologie, Hôpital Henri Mondor, Assistance Publique Hôpitaux de Paris, 94000 Créteil, France

^d Univ Paris Est Créteil, EpiDermE, Créteil, France

^e Reference center for toxic bullous dermatoses and severe drug reactions TOXIBUL, Créteil, France

^f Service de Pathologie, Hôpital Henri Mondor, Assistance Publique Hôpitaux de Paris, 94000 Créteil, France

^g Université Paris-Saclay, CNRS, Institut de Chimie Physique, 310 rue Michel Magat, 91400 Orsay, France

^h Sorbonne Université, Hôpital Tenon, Service des Explorations Fonctionnelles Multidisciplinaires, Paris, France

ⁱ Sorbonne Université, Hôpital Tenon, Service de Pathologie, Paris, France

^j Service de Réanimation médicale, Hôpital Henri Mondor, Assistance Publique Hôpitaux de Paris, 94000 Créteil, France

Current address: APHP, Service Plaies et Cicatrisation, Hôpital Rothschild, 5, Rue Santerre, 75012 Paris, France (H. Colboc)

E-mails: hester.colboc@aphp.fr (H. Colboc), thomas.bettuzzi@aphp.fr (T. Bettuzzi), marine.badrignans@aphp.fr (M. Badrignans), dominique.bazin@universite-paris-saclay.fr (D. Bazin), antoine.boury@universite-paris-saclay.fr (A. Boury), emmanuel.letavernier@tnn.aphp.fr (E. Letavernier), vincent.frochot@aphp.fr (V. Frochot), Ellieyali.tang@hotmail.com (E. Tang), philippe.moguelet@aphp.fr (P. Moguelet), nicolas.ortonne@aphp.fr (N. Ortonne), nicolas.de-prost@aphp.fr

* Corresponding authors.

Contributed equally.

(N. de Prost), saskia.oro@aphp.fr (S. Ingen-Housz-Oro), daudonmichel24@gmail.com (M. Daudon)

Abstract. Epidermal necrolysis (EN) is a rare life-threatening condition, usually drug-induced and characterised by a diffuse epidermal and mucosal detachment. Calcinosis cutis is reported in various skin diseases, occurring preferentially with tissue damage, but has never been described in EN. Clinical, biological and histopathological characteristics of three patients were retrospectively obtained from medical charts. Immunohistochemistry of classical osteogenic markers was used to explore the pathogenesis of the calcifications; their chemical composition was determined by μ Fourier transform infra-red (μ FTIR) spectroscopy and their localization and morphology by field-emission scanning electron microscopy (FE-SEM). In a recent letter, part of the results of this investigation has been already presented. In this contribution, we have added original data to this previous letter. We have investigated a set of biopsies corresponding to patients who presented atypical healing retardation due to calcinosis cutis. Through FE-SEM observations at the nanometre scale, we describe different areas where are present voluminous calcifications at the surface, submicrometre spherical entities within the papillary dermis and then large “normal” fibres. FE-SEM observations show clearly that “large” calcifications are the result of an agglomeration of small spherical entities. Moreover, micrometre scale spherical entities are the results of an agglomeration of nanometre scale spherical entities. Finally, the last set of data seems to show that the starting point of the calcifications process is “distant” from the epidermis in part of the dermis which appears undamaged. Regarding the chemical composition of large calcifications, different μ FTIR maps which underlined the presence of calcium-phosphate apatite have been gathered. Moreover, histopathology indicates that these pathological calcifications are not induced following a trans-differentiation of the skin cells into an osteochondrogenic phenotype. The association of caspofungin administration, known to induce in vitro intracellular calcium influx, and inflammation, induced by EN, known to favor dystrophic calcifications in various inflammatory skin diseases, could explain this never-before reported occurrence of calcinosis cutis.

Keywords. Epidermal necrolysis, Caspofungin, Pathological calcifications, Scanning electron microscopy, Fourier Transform Infrared Spectroscopy.

Published online: 20 July 2022

1. Introduction

Epidermal necrolysis (EN) (i.e., Stevens Johnson syndrome and toxic epidermal necrolysis (TEN) according to the extent of detached body surface area) is a rare life-threatening condition, usually drug-induced, characterised by a diffuse epidermal and mucosal detachment. Skin histology reveals pan epidermal necrolysis. Mucocutaneous healing usually lasts 2 to 3 weeks [1]. Bacterial or fungal infections, with skin as a portal of entry, are a main complication of the disease, especially in TEN [2,3].

As recalled by Le and Bedocs [4], calcinosis cutis is classified into five main types: dystrophic, metastatic, idiopathic, iatrogenic, and calciphylaxis. Dystrophic calcification is the most common cause and occurs preferentially with tissue damage. Little is known regarding the chemical composition of calcium salts associated to calcinosis cutis which are deposited in the skin and subcutaneous tissue.

From a chemical point of view, the chemical diversity of abnormal deposit in skin [5] with an exoge-

nous origin has been investigated in several papers dedicated for example to tattoo [6–9] or to sarcoidosis [10,11]. The chemical diversity of abnormal deposits in skin with an endogenous origin is less documented but has been underlined. In our case, for calcification of endogenous origin, we give evidence through physicochemical characterization techniques of the presence of calcium carbonate in the case of sarcoidosis [12,13] or of calcium phosphate apatite in the case of calcific uremic arteriopathy [14].

Such chemical diversity of pathological calcifications [15–21] calls for a characterization through physicochemical techniques such vibrational spectroscopies namely Fourier Transform Infra-Red (FTIR) or Raman spectroscopies [18,22–26] which are able to describe precisely their chemistry. Imaging through field-emission scanning electron microscopy (FE-SEM) coupled with an energy-dispersive X-ray (EDX) spectrometer have also to be performed to describe and localize precisely at the submicrometre scale such abnormal deposits [18,27–29].

Here we describe three patients who presented atypical healing retardation due to calcinosis cutis, a finding not previously described in EN. Part of the results presented in this investigation has been already published in a letter [30]. Here, a completely new set of unpublished data encompassing FE-SEM observations, EDX and μ FTIR measurements is presented in order to discuss more precisely the pathogenesis process related to calcinosis cutis.

2. Methods

The main characteristics of the three patients, admitted to the intensive care unit of our SJS/TEN reference centre between October, 2017 and February 2021, were retrospectively obtained from medical charts.

To investigate the origin and the composition of the epidermal calcifications, we conducted several experiments. For the hypothesis of calcium deposition induced by a trans-differentiation of fibroblasts or keratinocytes to an osteochondrogenic phenotype, immunohistochemistry was used to investigate classical osteogenic markers. Sections of paraffin-embedded skin biopsy, 4 μ m thick, were dewaxed, heated in citric acid solution (Target Retrieval Solution pH6, Dako), then incubated with antibodies. After blockade of endogenous peroxidase (peroxidase blocking solution, Dako), sections were immunostained with antibodies specific for the following osteogenic markers: bone morphogenic protein 2 (BMP-2, polyclonal, 1:300; Abcam), runt-related transcription factor 2 (Runx2, polyclonal, 1:200; GeneTex), alkaline phosphatase (monoclonal, 1:200; Abcam) and sclerostin (polyclonal, 1:100; Santa Cruz Biotechnology). Immunostaining was revealed by specific Histofin (Nichirei Biosciences) and AEC (k34769, Dako) staining.

Additional 4 μ m thick sections of paraffin-embedded skin biopsies were deposited on low-e microscope slides (MIRRIR, Kevley Technologies, Tienta Sciences, Indianapolis, IN, USA) for μ FTIR spectroscopy, FE-SEM observations and EDX measurements.

μ FTIR spectra have been collected by using a Spectrum Spotlight 400 imaging system (Perkin-Elmer Life Sciences), with 6.25 μ m spatial resolution and 8 cm^{-1} spectral resolution [22,23,30–32].

The concise description of the topology at the sub-micrometer scale of the sample is obtained using a FE-SEM (Zeiss SUPRA55-VP) microscope. High-resolution images were obtained with an Everhart-Thornley secondary electron detector. Measurements were taken at low voltage (less than 1 kV generally), without the usual carbon-coating of the sample surface. Finally, EDX spectroscopy was also used to identify the different elements present in the sample. Special attention has been taken to calcium and phosphorus in tissue [18,27–29].

3. Results and discussion

3.1. Clinical data

Regarding epidemiology, calcinosis cutis commonly occurs in patients with systemic sclerosis, especially the limited form (CREST syndrome). Twenty-five to forty percent of patients with limited systemic sclerosis will develop calcinosis cutis ten years after the onset of disease. Calcinosis cutis is seen in 30% of adults and up to 70% of children and adolescents with dermatomyositis. Patients with systemic lupus erythematosus can present with periarticular calcification in 33% of cases and soft tissue calcification in 17%.

Here we report three patients with severe TEN in whom secondary epidermal detachment with calcinosis cutis developed that was not previously described in this condition. This event was observed in the three cases a few days after caspofungin administration. One patient died and the two other patients presented an unusual, prolonged cutaneous healing. Clinical characteristics and histological results for the three patients are presented in Table 1.

Patient 1 was a 57 year-old woman, with TEN induced by pantoprazole. At day 6 after admission in our dermatology department, she was referred to ICU for a first septic shock to *P. aeruginosa* and *P. mirabilis*. On day 12 after admission, cutaneous healing was almost complete (Figure 1A). On day 18, she presented septic shock with *Candida parapsilosis* bloodstream infection and received caspofungin for 14 days. On day 29, dermatological examination revealed a diffuse epidermal detachment associated with atone fibrinous plaques (Figure 1B). Thereafter, the evolution was slowly favourable and the patient

Table 1. Clinical and demographic data of three patients admitted to the intensive care unit for toxic epidermal necrolysis

	Patient 1	Patient 2	Patient 3
Age	57	49	59
Sex	Female	Male	Male
Drug culprit of the TEN	Pantoprazole	Ibuprofen	Allopurinol
SCORTEN ^a at admission	2	4	3
Maximal body surface area involved	100%	100%	80%
Cutaneous biopsy at admission	Epidermal necrolysis	Epidermal necrolysis	Epidermal necrolysis
Time between caspofungin administration and abnormal epidermal detachment ^b	8 days	1 day	3 days
Cutaneous biopsy at epidermal detachment	Necrosis of the corneal layer associated with calcium deposition in the superficial dermis and epidermis	Necrosis of the corneal layer associated with calcium deposition in the superficial dermis	Necrosis of the corneal layer associated with calcium deposition in the superficial dermis
Type of delayed cutaneous healing	Relapse of fibrinous erosions 17 days after complete healing	Extension of fibrinous erosions 3 days after the beginning of healing	Relapse of cutaneous erosions 22 days after complete healing
Topography of detachment	Anterior trunk and limbs	Limbs, trunk	Upper trunk, shoulders, back
Time to complete healing	166 days	Not available (died at day 33)	Not obtained at day 156

^a SCORTEN is a specific severity-of-illness score for TEN, ranging from 0 to ≥ 5 . A high SCORTEN is associated to a higher mortality rate.

^b As defined by the day it was evidenced by the dermatologist.

was discharged from the ICU. Complete healing occurred 166 days after the second epidermal detachment.

Patient 2 was a 49 year-old man TEN with ibuprofen suspected. He was transferred to ICU because of respiratory distress. At day 3 after admission in ICU, he showed places of beginning of healing. On day 5, he presented non-documented septic shock and received vancomycin, piperacillin-tazobactam and caspofungin. On day 6, diffuse epidermal detachment was noted, together with extended fibrinous areas. He died on day 33 of multiple organ failure, without healing of fibrinous plaques.

Patient 3 was a 59 year-old male with TEN induced by allopurinol. He was transferred in the ICU and

was rapidly treated with piperacilline-tazobactam for *Klebsiella aerogenes* pneumonia. On day 12 after admission, cutaneous healing was almost complete. The same day, caspofungin was administered for *Candida lusitaniae* catheter infection, with fluconazole relay 2 days later. On day 26, the patient presented a septic shock to *Candida parapsilosis*. Caspofungin was reintroduced for 2 days, followed by fluconazole for 12 more days. On day 34, dermatological examination revealed a diffuse epidermal detachment with extended atone fibrinous areas. On day 156, complete mucocutaneous healing still had not occurred.

In the three cases, skin biopsy performed at diagnosis revealed epidermal necrosis typical of EN [33].



Figure 1. Clinical presentation of patient 1, showing delayed healing with prolonged erosions covered with yellowish crusts.

In light of healing retardation, a new biopsy revealed diffuse necrosis of the corneal layer associated with calcium deposition in the superficial dermis and in the epidermis, which was confirmed by Von Kossa staining (Figure 2A). Median ionized calcium was 1.19 (0.97–1.25) mmol/L (normally 1.15–1.33). No patient had received calcium supplementation. Median phosphoremia was 0.89 mmol/L (normally 0.61–1.11 mmol/L). Phosphate supplementation was administered in routine care [1]. The three patients received caspofungin for fungal sepsis, a rare infectious event in EN.

On retrospectively reviewing all patients ($n = 115$) in our centre between January, 2015 and December, 2020, four other patients with TEN had also received caspofungin: three had died in the following days without any dermatological examination. In the fourth case, new fibrinous plaques were described in the medical chart 4 days after caspofungin administration (no imaging or histology performed).

Caspofungin is an inhibitor of the β -D glucan synthesis of fungal pathogens [34]. Nonetheless, caspofungin is also a proven agonist of ryanodine receptor (RyR), found on cardiomyocytes and on pulmonary epithelial cells, inducing intracellular calcium influx from endoplasmic reticulum to cytosol [35,36]. Although the effect of caspofungin on keratinocytes

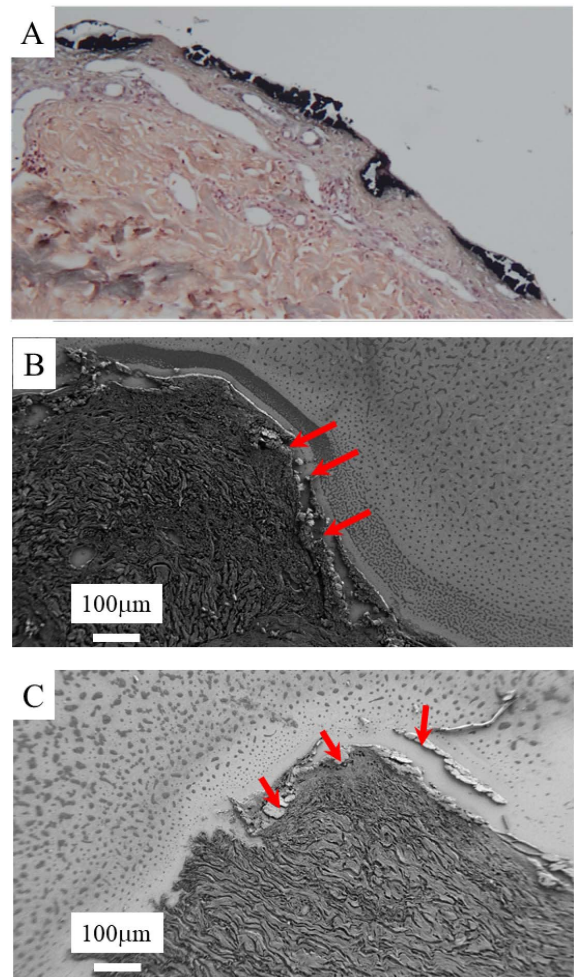


Figure 2. Skin biopsy sections. Diffuse necrosis of the corneal layer associated with calcium deposition in the superficial dermis. A, Von Kossa staining ($\times 100$). B and C, FE-SEM observations at low magnification. Red arrows indicate the voluminous calcifications.

has not been studied, Denda *et al.* [37] reported that RyR is strongly expressed in keratinocytes and that the application of another RyR agonist induced intracellular calcium flux, leading to a precocious keratinocyte differentiation in an *in vitro* model and a delayed cutaneous healing in a mouse model. All osteogenic markers were negative on keratinocytes as on fibroblasts, excluding a trans-differentiation to an osteochondrogenic phenotype.

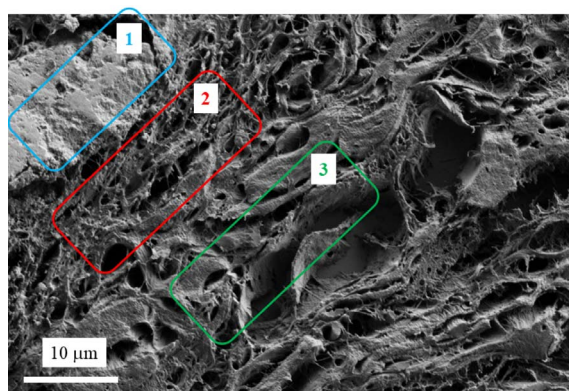


Figure 3. Skin biopsy sections as seen with a FE-SEM at higher magnification. A and B voluminous calcification (inside the blue rectangle) and spherical calcifications within the papillary dermis.

3.2. The three different areas as defined by SEM observations

FE-SEM revealed that these deposits consisted of voluminous plaques (Figures 2B and C). FE-SEM observations at higher magnification (Figure 3) underline the presence of the voluminous plaques (area 1 in Figure 3). Just below, we can see spherical entities within the papillary dermis (area 2 in Figure 3). Finally, an area which seems to be free of calcification can be defined (area 3 in Figure 3).

In order to gather information regarding the chemistry of the abnormal deposits, we have performed EDX and μ FTIR. Figure 4 shows three EDX spectra. In the first one corresponding to the support, different elements are identified, namely O ($K_{\alpha 1} = 0.524$ KeV), Zn ($K_{\alpha 1} = 8.638$ KeV, $K_{L1} = 1.011$ KeV), Si ($K_{\alpha 1} = 1.740$ KeV), P ($K_{\alpha 1} = 2.013$ KeV), Ag ($L_{\alpha 1} = 2.985$ KeV, $L_{\beta 1} = 3.150$ KeV), K ($K_{\alpha 1} = 3.310$ KeV) and Ca ($K_{\alpha 1} = 3.690$ KeV, $K_{\beta 1} = 4.010$ KeV) [38,39]. In EDX spectra (red line in Figure 4) related to the large calcification (area 1 in Figure 3), contribution coming from some elements present in the support namely Si, Ag, K and Zn are no more visible. Instead, contributions of Ca and P are associated with a strong amplitude. Note that the X-ray fluorescence peak at 1.0 KeV corresponds to a sum peak (star in Figure 4) due to the coincidence of two O $K_{\alpha 1}$ photons. Finally, in EDX spectra (blue

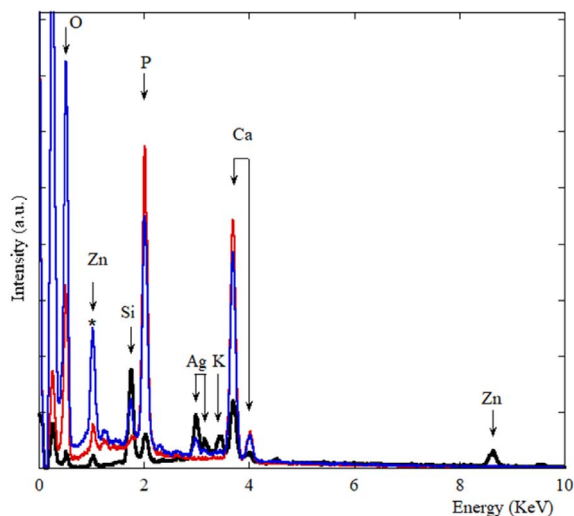


Figure 4. EDX spectra of the support (black line), calcification 1 (red line) and spherical entities which belong to calcification 2 (blue line). We can see the different contributions coming from the support namely O ($K_{\alpha 1} = 0.524$ KeV), Zn ($K_{\alpha 1} = 8.638$ KeV, $K_{L1} = 1.011$ KeV), Si ($K_{\alpha 1} = 1.740$ KeV), P ($K_{\alpha 1} = 2.013$ KeV), Ag ($L_{\alpha 1} = 2.985$ KeV, $L_{\beta 1} = 3.150$ KeV), K ($K_{\alpha 1} = 3.310$ KeV) and Ca ($K_{\alpha 1} = 3.690$ KeV, $K_{\beta 1} = 4.010$ KeV).

line in Figure 4) related to the spherical calcifications (area 2 in Figure 3), contributions of Ca and P related to the calcifications and of other elements present in the support are measured.

On Figure 5, μ FTIR spectra corresponding to large calcifications (red line in Figure 5) and tissue (black line in Figure 5) are visualized. μ FTIR spectroscopy revealed that calcifications consisted of amorphous calcium phosphate and calcium-phosphate apatite which is consistent with the composition of most dystrophic skin calcifications [40–43].

3.3. The pathogenesis of large calcifications

On Figure 6, we can see that “large” submillimeter scale calcifications are the result of an agglomeration of micrometer scale spherical entities. Such fusion process of spherical entities leading to “large” submillimeter scale calcifications has been also observed in other organs such breast [44].

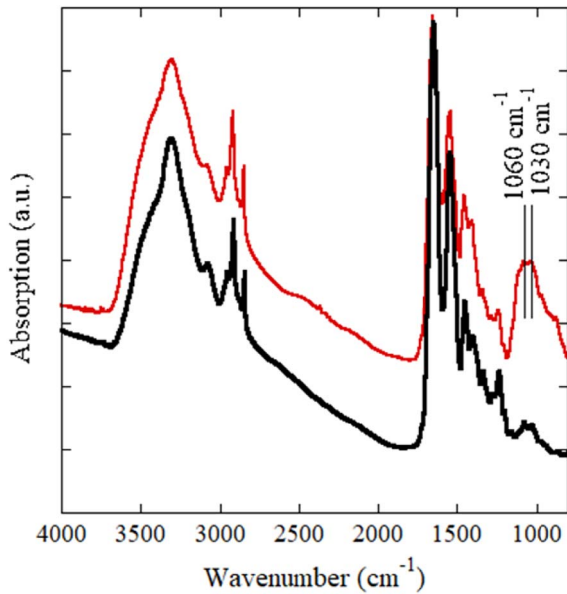


Figure 5. μ Fourier transform infra-red spectroscopy of calcium deposition. The presence of amorphous calcium phosphate and calcium phosphate apatite spectrum with characteristic peaks (1060 cm^{-1} and 1030 cm^{-1}) in a protein matrix (skin tissue) is detected.

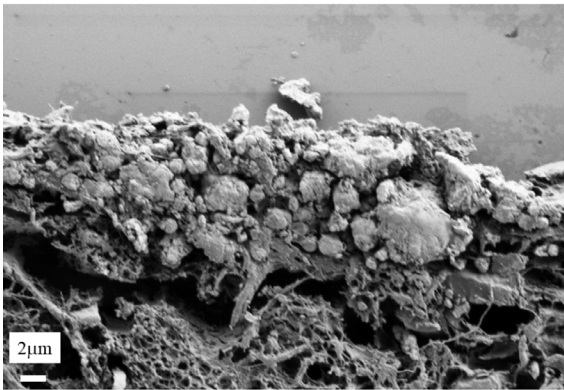


Figure 6. Area 1 is made of “large” calcifications (area 1 in Figure 3) which are the result of an agglomeration of small spherical entities (area 2 in Figure 3).

3.4. *The pathogenesis of micrometer spherical entities*

It is worth to underline that the internal structure of spherical entities may display different configuration as we have shown previously in the case of an investigation dedicated to breast calcifications (Figure 7) [44].

3.5. *The very first steps of the pathogenesis of micrometer spherical entities*

Finally, we have tried to localize precisely the very first steps of the calcification process. In Figure 8, we can see a set of nanometre scale spherical entities without micrometre spherical ones. It seems that the organisation of the skin is altered by the presence of the nanospherical calcifications. Intermingled tiny fibres are clearly visible around these calcifications and might be reticulin. Note that ectopic presence of reticulin has been found in pseudoxanthoma elasticum, a genetic calcifying skin disorders, suggesting the existence of a tropism of the calcification for such kind of fibres [45].

3.6. *Physiological and biochemical considerations*

The presence of spherical calcified entities within the upper but not deeper dermis suggests that these calcifications formed in the upper part of the skin tissue, contiguous to the epidermal necrosis. Such co-location suggests a link between inflammation induced by the EN and calcifications, as in other dystrophic calcified skin diseases such as dermatomyositis [46,47].

Regarding the pathogenesis of these calcifications, caspofungin administration might have disrupted the extracellular/intracellular gradient of calcium in keratinocytes, causing an extracellular calcium deposit, associated with secondary epithelial detachment in these patients with previous skin fragility (ongoing TEN healing) and prolonged inflammation. Because of the negativity of osteogenic markers in all three patients, the hypothetical mechanism of trans-differentiation of fibroblasts or keratinocytes to an osteochondrogenic phenotype, as suspected with vascular smooth muscle cells of dermal arterioles in calciphylaxis, seems unlikely [48]. We acknowledge

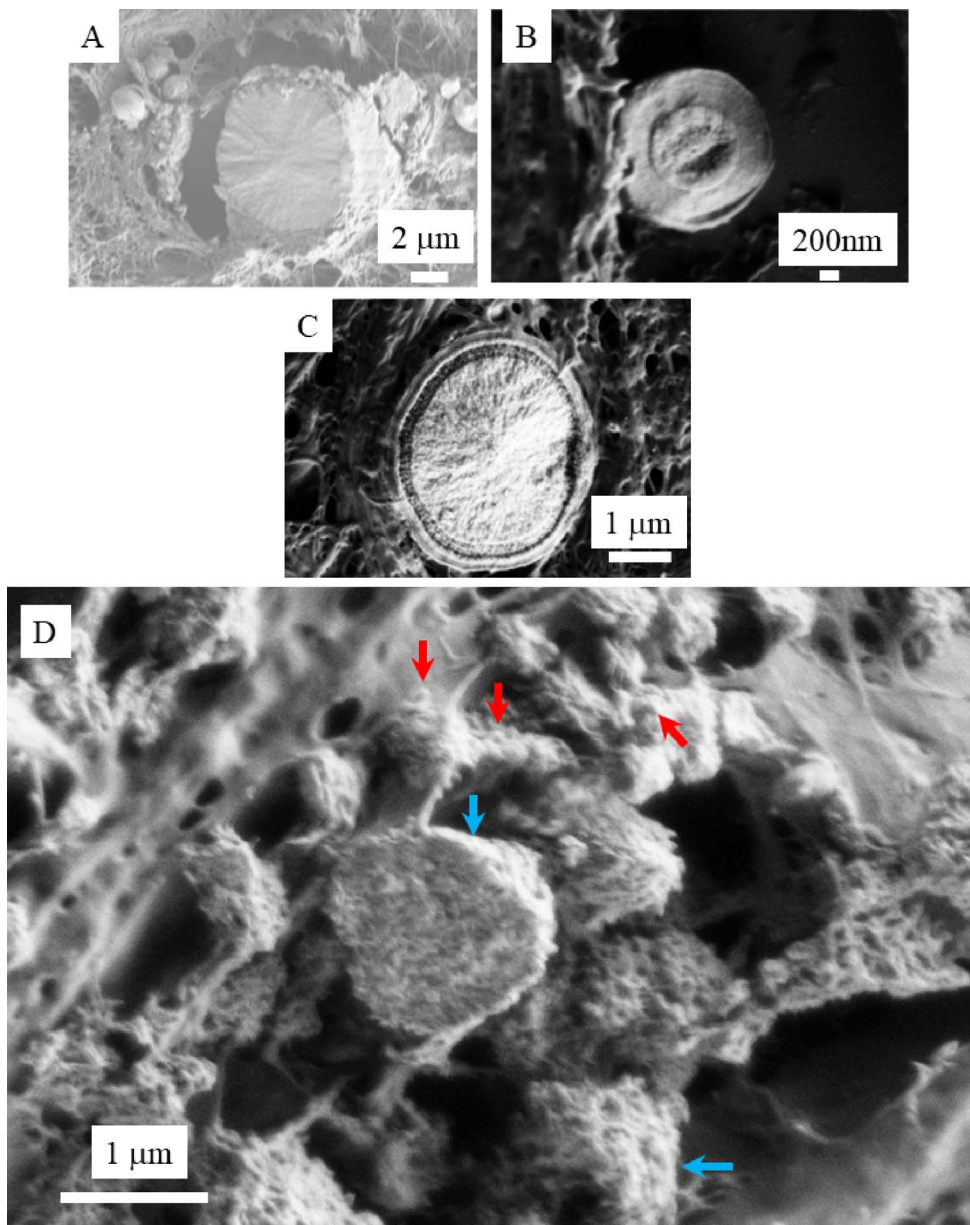


Figure 7. Spherical entities may display different internal structures: (A) Radial structures; (B): Concentric layers; (C): Both radial and concentric structure (A to C images are breast calcifications). In the case of calcinosis cutis (D), microspherical entities (blue arrows) result of an agglomeration of nano-spherules (red arrows).

some limitations of the study. The first is the retrospective design associated with a limited number of patients and the absence of a control arm. Moreover, we did not use an *in vitro* model of the possible

pathogenesis link between calcification and caspofungin. Nonetheless, the occurrence of the same situation in three similar patients after caspofungin administration associated with a possible pathogenesis

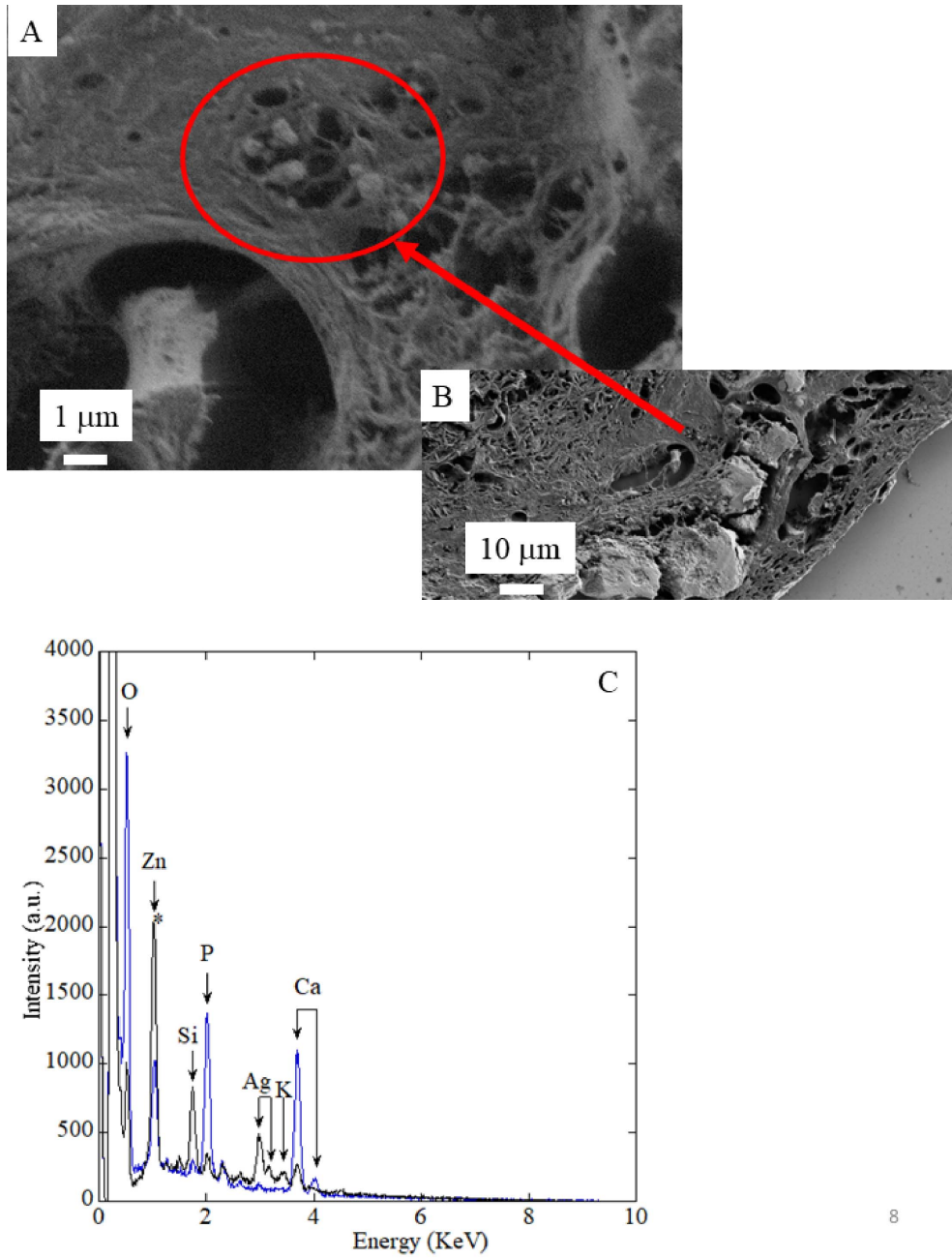


Figure 8. (A, B) Spherical entities as seen at two magnifications; (C) black line corresponds to the EDX spectra of the support and blue line corresponds to spherical entities visible in (A).

hypothesis raises the possible causality of caspofungin. Liposomal amphotericin B or fluconazole might therefore be preferred for patients with TEN in case of invasive fungal infection.

4. Conclusion

We have investigated a set of biopsies corresponding to patients who presented atypical healing retardation due to calcinosis cutis. Through SEM observations at the nanometer scale, we describe different areas: voluminous calcifications present at the surface of the skin tissue, submicrometer spherical entities within the papillary dermis and then normally structured dermal fibers. FE-SEM observations show clearly that “large” calcifications are the result of an agglomeration of micrometer spherical entities. Moreover, micrometer scale spherical entities are the results of an agglomeration of nanometer scale spherical entities. Finally, the last set of data seems to show that the starting point of the calcifications process is “distant” from the epidermis in part of the dermis which appears undamaged.

From a medical point of view, our cases alert to the administration of caspofungin in patients presenting diffuse epidermal detachment and pave the way for further studies regarding dermatological adverse events induced by caspofungin, especially on mucocutaneous healing.

Conflicts of interest

Authors have no conflict of interest to declare.

Acknowledgment

The patients in this manuscript have given written informed consent to publication of their case details.

References

- [1] S. Ingen-Housz-Oro, T.-A. Duong, B. Bensaid, N. Bellon, N. de Prost, D. Lu, B. Lebrun-Vignes, J. Gueudry, E. Bequignon, K. Zaghbib, G. Royer, A. Colin, G. Do-Pham, Ch. Bodemer, N. Ortonne, A. Barbaud, L. Fardet, O. Chosidow, P. Wolkenstein, *Orphanet J. Rare Dis.*, 2018, **13**, article no. 56.
- [2] T. A. Duong, L. Valeyrie-Allanore, P. Wolkenstein, O. Chosidow, *The Lancet*, 2017, **390**, 1996-2011.
- [3] A. Lecadet, P.-L. Woerther, C. Hua, A. Colin, C. Gomart, J.-W. Decousser, A. MekontsoDessap, P. Wolkenstein, O. Chosidow, N. de Prost, S. Ingen-Housz-Oro, *J. Am. Acad. Dermatol.*, 2019, **81**, 342-347.
- [4] C. Le, P. M. Bedocs, “Calcinosis cutis”, in *StatPearls [Internet]*, StatPearls Publishing, Treasure Island, FL, 2021, [Updated 2021 Jul 17]. Available from: <https://www.ncbi.nlm.nih.gov/books/NBK448127/>.
- [5] H. Colboc, Ph. Moguelet, E. Letavernier, V. Frochot, J.-F. Bernaudin, R. Weil, S. Rouzière, P. Senet, C. Bachmeyer, N. Laporte, I. Lucas, V. Descamps, R. Amode, F. Brunet-Possenti, N. Kluger, L. Deschamps, A. Dubois, S. Reguer, A. Somogyi, K. Medjoubi, M. Refregiers, M. Daudon, D. Bazin, *C. R. Chim.*, 2022, **25**, no. S1, 445-476.
- [6] H. Colboc, D. Bazin, P. Moguelet, S. Reguer, R. Amode, C. Jouanneau, I. Lucas, L. Deschamps, V. Descamps, N. Kluger, *J. Eur. Acad. Dermatol. Venereol.*, 2020, **34**, e313-e315.
- [7] G. Forte, F. Petrucci, A. Cristaudo, B. Bocca, *Sci. Total Environ.*, 2009, **407**, 5997-6002.
- [8] M. Arl, D. J. Nogueira, J. Sch. Köerich, N. M. Justino, D. S. Vicentini, W. G. Matias, *J. Hazard. Mater.*, 2019, **364**, 548-561.
- [9] H. Colboc, D. Bazin, P. Moguelet, S. Reguer, R. Amode, C. Jouanneau, I. Lucas, L. Deschamps, V. Descamps, N. Kluger, *J. Synchrotron Radiat.*, submitted.
- [10] L. Ch. Oliver, A. M. Zarnke, *Chest*, 160, **2021**, 1360-1367.
- [11] L. S. Newman, C. S. Rose, E. A. Bresnitz, M. D. Rossman, J. Barnard, M. Frederick, M. L. Terrin, S. E. Weinberger, D. R. Moller, G. McLennan, G. Hunninghake, L. DePalo, R. P. Baughman, M. C. Iannuzzi, M. A. Judson, G. L. Knatterud, B. W. Thompson, A. S. Teirstein, H. Yeager Jr., C. J. Johns, D. L. Rabin, B. A. Rybicki, R. Cherniack, *Am. J. Respir. Crit. Care Med.*, 170, **2004**, 1324-1330, ACCESS Research Group.
- [12] H. Colboc, D. Bazin, Ph. Moguelet, V. Frochot, R. Weil, E. Letavernier, Ch. Jouanneau, C. Frances, C. Bachmeyer, J.-F. Bernaudin, M. Daudon, *C. R. Chim.*, 2016, **19**, 1631-1641.
- [13] H. Colboc, P. Moguelet, D. Bazin, C. Bachmeyer, V. Frochot, R. Weil, E. Letavernier, C. Jouanneau, M. Daudon, J.-F. Bernaudin, *J. Eur. Acad. Dermatol. Venereol.*, 2019, **33**, 198-203.
- [14] H. Colboc, Ph. Moguelet, D. Bazin, P. Carvalho, A.-S. Dillies, G. Chaby, H. Maillard, D. Kottler, E. Goujon, Ch. Jurus, M. Panaye, V. Frochot, E. Letavernier, M. Daudon, I. Lucas, R. Weil, Ph. Courville, J.-B. Monfort, F. Chasset, P. Senet, *JAMA Dermatol.*, 2019, **155**, 789-796.
- [15] D. Bazin, M. Daudon, C. Combes, C. Rey, *Chem. Rev.*, 2012, **112**, 5092-5120.
- [16] D. Bazin, M. Daudon, *J. Phys. D: Appl. Phys.*, 2012, **45**, article no. 383001.
- [17] L. N. Poloni, M. D. Ward, *Chem. Mater.*, 2014, **26**, 477-495.
- [18] D. Bazin, M. Daudon, *Ann. Biol. Clin.*, 2015, **73**, 517-534.
- [19] S. R. Mulay, H.-J. Anders, *N. Engl. J. Med.*, 2016, **374**, 2465-2476.
- [20] M. Li, J. Zhang, L. Wang, B. Wang, Ch. V. Putnis, *J. Phys. Chem. B*, 2018, **122**, 1580-1587.
- [21] E. Tsolaki, S. Bertazzo, *Materials*, 2019, **12**, article no. 3126.
- [22] M. Daudon, D. Bazin, *C. R. Chim.*, 2016, **19**, 1416-1423.
- [23] D. Bazin, Ch. Jouanneau, S. Bertazzo, Ch. Sandt, A. Desombz, M. Réfrégiers, P. Dumas, J. Frederick, J.-Ph. Haymann,

- E. Letavernier, P. Ronco, M. Daudon, *C. R. Chim.*, 2016, **19**, 1439-1454.
- [24] D. Bazin, E. Letavernier, J. P. Haymann, V. Frochot, M. Daudon, *Ann. Biol. Clin.*, 2020, **78**, 349-362.
- [25] I. T. Lucas, D. Bazin, M. Daudon, *C. R. Chim.*, 2022, **25**, no. S1, 83-103.
- [26] S. Tamosaityte, M. Pucetaite, A. Zelvy, S. Varvuolyte, V. Hendrixson, V. Sablinskas, *C. R. Chim.*, 2022, **25**, no. S1, 73-72.
- [27] F. Brisset, *Microscopie Électronique à Balayage et Microanalyses*, EDP Sciences, Paris, France, 2012.
- [28] M. Racek, J. Racek, I. Hupáková, *Scand. J. Clin. Lab. Invest.*, 2019, **79**, 208-217.
- [29] D. Bazin, E. Boudierlique, M. Daudon, V. Frochot, J.-Ph. Haymann, E. Letavernier, F. Tielens, R. Weil, *C. R. Chim.*, 2022, **25**, no. S1, 37-60.
- [30] H. Colboc, T. Bettuzzi, M. Badrignans, D. Bazin, A. Boury, E. Letavernier, V. Frochot, E. Tang, P. Moguelet, N. Ortonne, N. de Prost, S. Ingen-Housz-Oro, *J. Eur. Acad. Dermatol. Venereol.*, 2022, **36**, e313-e315.
- [31] D. Bazin, M. Daudon, *J. Spectr. Imaging*, 2019, **8**, article no. a16.
- [32] D. Bazin, J.-Ph. Haymann, E. Letavernier, J. Rode, M. Daudon, *Presse Med.*, 2014, **43**, 135-148.
- [33] L. Valerie-Allanore, S. Bastuji-Garin, S. Guégan, N. Ortonne, M. Bagot, J.-C. Roujeau, J. E. Revuz, J. Wechsler, P. Wolkenstein, *J. Am. Acad. Dermatol.*, 2013, **68**, e29-e35.
- [34] P. L. McCormack, C. M. Perry, *Drugs*, 2005, **65**, 2049-2068.
- [35] S. Müller, C. Koch, S. Weiterer, M. A. Weigand, M. Sander, M. Henrich, *Sci. Rep.*, 2020, **10**, article no. 11723.
- [36] C. Koch, J. Jersch, E. Schneck, F. Edinger, H. Maxeiner, F. Uhle, M. A. Weigand, M. Markmann, M. Sander, M. Henrich, *Antimicrob. Agents Chemother.*, 2018, **62**, e01114-e01118.
- [37] S. Denda, J. Kumamoto, K. Takei, M. Tsutsumi, H. Aoki, M. Denda, *J. Invest. Dermatol.*, 2012, **132**, 69-75.
- [38] S. Rouzière, D. Bazin, M. Daudon, *C. R. Chim.*, 2016, **19**, 1404-1415.
- [39] D. Bazin, E. Foy, S. Reguer, S. Rouzière, B. Fayard, H. Colboc, J.-Ph. Haymann, M. Daudon, C. Mocuta, *C. R. Chim.*, 2022, **25**, no. S1, 165-188.
- [40] J. C. Elliott, *Structure and Chemistry of the Apatites and other Calcium Orthophosphates*, Elsevier, Amsterdam, 1994.
- [41] C. Combes, C. Rey, *Minerals*, 2016, **6**, article no. 34.
- [42] D. Eichert, C. Drouet, H. Sfiha, C. Rey, C. Combes, "Nanocrystalline apatite-based biomaterials: synthesis, processing and characterization", in *Trends in Biomaterials Research* (J. Patrick, ed.), Nova Science Publishers Inc., Pannone, 2007.
- [43] N. Reiter, L. El-Shabrawi, B. Leinweber, A. Berghold, E. Aberer, *J. Am. Acad. Dermatol.*, 2011, **65**, 1-12.
- [44] A. Ben Lakhdar, M. Daudon, M. C. Matthieu, A. Kellum, C. Balleuquier, D. Bazin, *C. R. Chim.*, 2016, **19**, 1610-1624.
- [45] L. Danielsen, T. Kobayasi, H. W. Larsen, K. Midtgaard, H. E. Christensen, *Acta Derm. Venereol.*, 1970, **50**, 355-373.
- [46] H. Colboc, Ph. Moguelet, D. Bazin, A. Croué, V. Frochot, M. Daudon, R. Weil, E. Letavernier, L. Martin, *Annales de Dermatologie et de Vénérologie*, 2019, **146**, article no. A202.
- [47] G. Munavalli, A. Reisenauer, M. Moses, S. Kilroy, J. L. Arbiser, *J. Dermatol.*, 2003, **30**, 915-919.
- [48] S. U. Nigwekar, R. Thadhani, V. M. Brandenburg, *N. Engl. J. Med.*, 2018, **378**, 1704-1714.